- Rotaxanes and Biofunctionalized Pseudorotaxanes via Thiol-Maleimide Click Chemistry
  Choudhary, U.; Northrop, B. H. *Org. Lett.* **2012**, *14*, 2082-2085.
  Abstract:

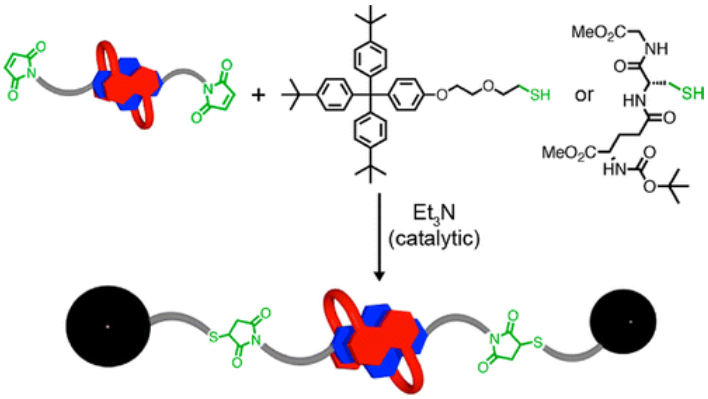

Base-catalyzed thiol-maleimide click chemistry has been applied to the synthesis of neutral donor–acceptor [2]rotaxanes in good yield. This method is extended further to the synthesis of a glutathione-functionalized [2]pseudorotaxane, a precursor to integrated conjugates of interlocked molecules with proteins and enzymes.

- A New "Turn-on" Naphthalenedimide-Based Chemosensor for Mercury Ions with High Selectivity: Successful Utilization of the Mechanism of Twisted Intramolecular Charge Transfer, Near-IR Fluorescence, and Cell Images
  Li, Q.; Peng, M.; Li, H.; Zhong, C.; Zhang, L.; Cheng, X.; Peng, X.; Wang, Q.; Qin, J.; Li, Z. *Org. Lett.* **2012**, *14*, 2094-2097.
  Abstract:

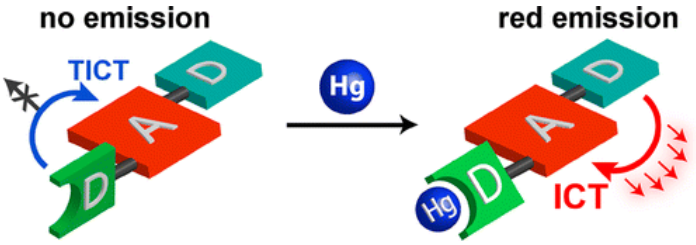

For the first time, a new near-IR "turn-on" fluorescent chemosensor with high selectivity for Hg^{2+} ions was designed according to the twisted intramolecular charge transfer (TICT) mechanism. The selective fluorescence enhancement effect can be optimized by modulating the solvent systems. And this naphthalenedimide-based sensor with long wavelength absorption and emission can be used to image intracellular Hg^{2+} ions in living Hela cells.

- Synthesis, Electronic, and Morphological Properties of Tetrahedral Oligothiophenes with *n*-Hexyl Terminal Groups
  Matsumoto, K.; Kugo, S.; Takajo, D.; Inaba, A.; Hirao, Y.; Kurata, H.; Kawase, T.; Kubo, T. *Chem. Asian J.* **2012**, *7*, 225–232.
  Abstract:

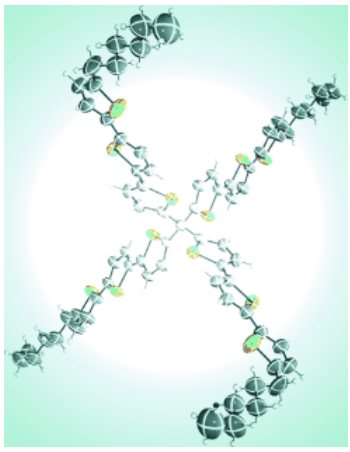

A series of tetrahedral oligothiophenes bearing *n*-hexyl groups at the α-positions of the terminal thiophene rings, $(n\text{-}C_6H_{13}(C_4H_2S)_n)_4C$ (Hex-T*n*TM; *n*=1–4), has been synthesized by Kosugi–Migita–Stille coupling as a key reaction. Thanks to the improved solubility afforded by the terminal *n*-hexyl groups, the largest homologue (*n*=4) was successfully obtained. Whereas the smaller derivatives (*n*=1, 2) were obtained as liquid substances, the larger derivatives (*n*=3, 4) were obtained as solids. Hex-T3 TM partially adopts *syn* conformations between the adjacent thiophene rings in the crystal, probably owing to the packing force. Hex-T3 TM not only appeared in the crystalline state but also the amorphous state, which was stable to up to 80 °C. Regardless of the terminal groups, the derivatives of *n*=2 exhibited a broad fluorescence with large Stokes shifts compared to the corresponding linear analogues, thereby suggesting the presence of intramolecular interactions between the bithiophene moieties. Interactions between terthiophene branches was also suggested in the radical cations of Hex-T3 TM by cyclic voltammetry measurements.

- Chronological Change from Face-On to Edge-On Ordering of Zinc–Tetraphenylporphyrin at the Phenyloctane–Highly Oriented Pyrolytic Graphite Interface
  Sakano, T.; Hasegawa, J.-Y.; Higashiguchi, K.; Matsuda, K. *Chem. Asian J.* **2012**, *7*, 394–399.
  Abstract:

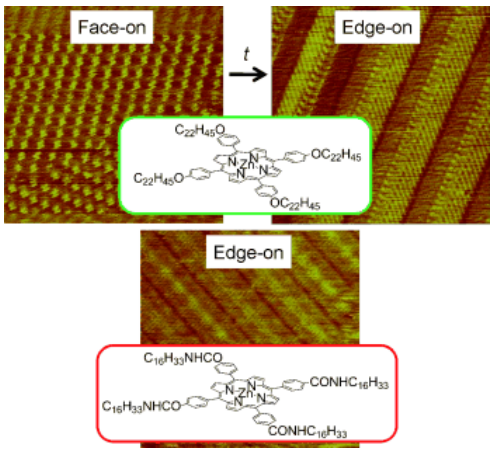

The self-assembled structure of alkoxy- and *N*-alkylcarbamoyl-substituted zinc–tetraphenylporphyrin at the liquid–highly oriented pyrolytic graphite (HOPG) interface was observed by using scanning tunneling microscopy. The alkoxy porphyrin showed a phase transition from face-on to edge-on ordering. The phase transition requires the close-packed structure of alkoxy porphyrin. The chronological change of the ordering was traced to show the existence of several types of Ostwald ripening including two-step phase transition from small edge-on to face-on and then further to edge-

on orderings. On the other hand, the *N*-alkylcarbamoyl porphyrin showed persistent edge-on ordering, and the ordering was analyzed by the Moiré pattern. Although the edge-on ordering is observed only in the nonpolar solvent, the orderings have potential applications in the charge and energy transfer.

- Self-Assembly of Flexible β-Strands into Immobile Amyloid-Like β-Sheets in Membranes As Revealed by Solid-State ^{19}F NMR
  Wadhwani, P.; Strandberg, E.; Heidenreich, N.; Bürck, J.; Fanghänel, S.; Ulrich, A. S. *J. Am. Chem. Soc.* **2012**, *134*, 6512–6515.
  Abstract:

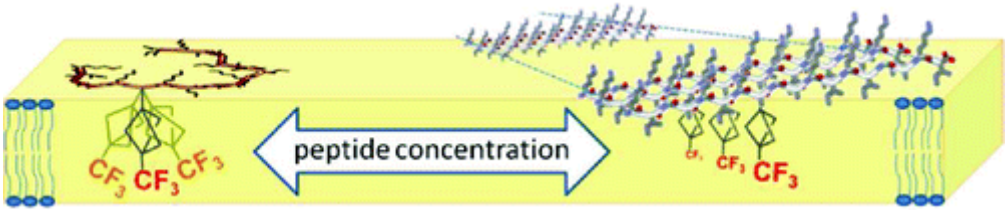

The cationic peptide $[KIGAKI]_3$ was designed as an amphiphilic β-strand and serves as a model for β-sheet aggregation in membranes. Here, we have characterized its molecular conformation, membrane alignment, and dynamic behavior using solid-state ^{19}F NMR. A detailed structure analysis of selectively ^{19}F-labeled peptides was carried out in oriented DMPC bilayers. It showed a concentration-dependent transition from monomeric β-strands to oligomeric β-sheets. In both states, the rigid ^{19}F-labeled side chains project straight into the lipid bilayer but they experience very different mobilities. At low peptide-to-lipid ratios ≤1:400, monomeric $[KIGAKI]_3$ swims around freely on the membrane surface and undergoes considerable motional averaging, with essentially uncoupled /ψ torsion angles. The flexibility of the peptide backbone in this 2D plane is reminiscent of intrinsically unstructured proteins in 3D. At high concentrations, $[KIGAKI]_3$ self-assembles into immobilized β-sheets, which are untwisted and lie flat on the membrane surface as amyloid-like fibrils. This is the first time the transition of monomeric β-strands into oligomeric β-sheets has been characterized by solid-state NMR in lipid bilayers. It promises to be a valuable approach for studying membrane-induced amyloid formation of many other, clinically relevant peptide systems.

- Structure of Triplex DNA in the Gas Phase
  Arcella, A.; Portella, G.; Ruiz, M. L.; Eritja, R.; Vilaseca, M.; Gabelica, V.; Orozco, M. *J. Am. Chem. Soc.* **2012**, *134*, 6596–6606.
  Abstract:

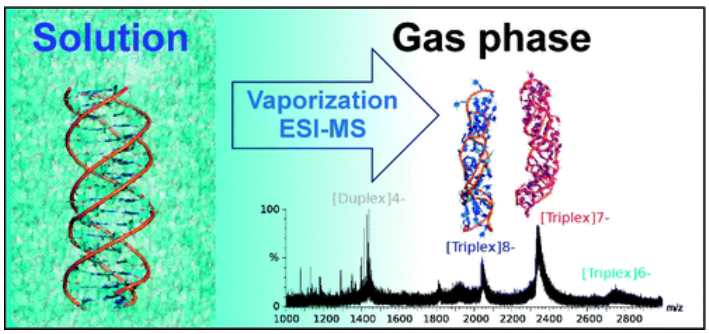

Extensive (more than 90 microseconds) molecular dynamics simulations complemented with ion-mobility mass spectrometry experiments have been used to characterize the conformational ensemble of DNA triplexes in the gas phase. Our results suggest that the ensemble of DNA triplex

structures in the gas phase is well-defined over the experimental time scale, with the three strands tightly bound, and for the most abundant charge states it samples conformations only slightly more compact than the solution structure. The degree of structural alteration is however very significant, mimicking that found in duplex and much larger than that suggested for G-quadruplexes. Our data strongly supports that the gas phase triplex maintains an excellent memory of the solution structure, well-preserved helicity, and a significant number of native contacts. Once again, a linear, flexible, and charged polymer as DNA surprises us for its ability to retain three-dimensional structure in the absence of solvent. Results argue against the generally assumed roles of the different physical interactions (solvent screening of phosphate repulsion, hydrophobic effect, and solvation of accessible polar groups) in modulating the stability of DNA structures.

- Implanted Biofuel Cell Operating in a Living Snail
  Halámková, L.; Halámek, J.; Bocharova, V.; Szczupak, A.; Alfonta, L.; Katz, E. *J. Am. Chem. Soc.* **2012**, *134*, 5040–5043.
  Abstract:

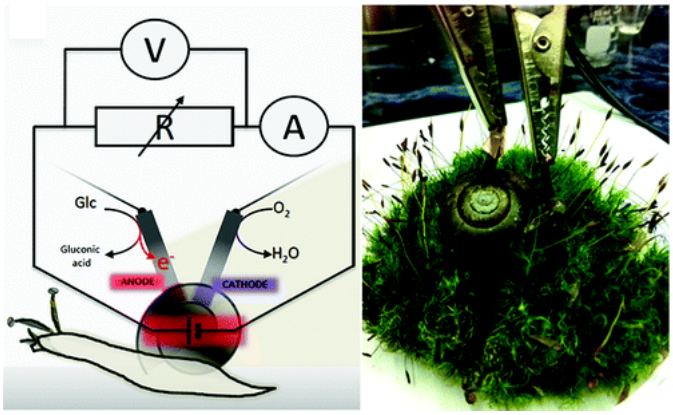

Implantable biofuel cells have been suggested as sustainable micropower sources operating in living organisms, but such bioelectronic systems are still exotic and very challenging to design. Very few examples of abiotic and enzyme-based biofuel cells operating in animals in vivo have been reported. Implantation of biocatalytic electrodes and extraction of electrical power from small living creatures is even more difficult and has not been achieved to date. Here we report on the first implanted biofuel cell continuously operating in a snail and producing electrical power over a long period of time using physiologically produced glucose as a fuel. The “electrified” snail, being a biotechnological living “device”, was able to regenerate glucose consumed by biocatalytic electrodes, upon appropriate feeding and relaxing, and then produce a new “portion” of electrical energy. The snail with the implanted biofuel cell will be able to operate in a natural environment, producing sustainable electrical micropower for activating various bioelectronic devices.

- Solid-State NMR Crystallography through Paramagnetic Restraints
  Luchinat, C.; Parigi, G.; Ravera, E.; Rinaldelli, M. *J. Am. Chem. Soc.* **2012**, *134*, 5006–5009.
  Abstract:

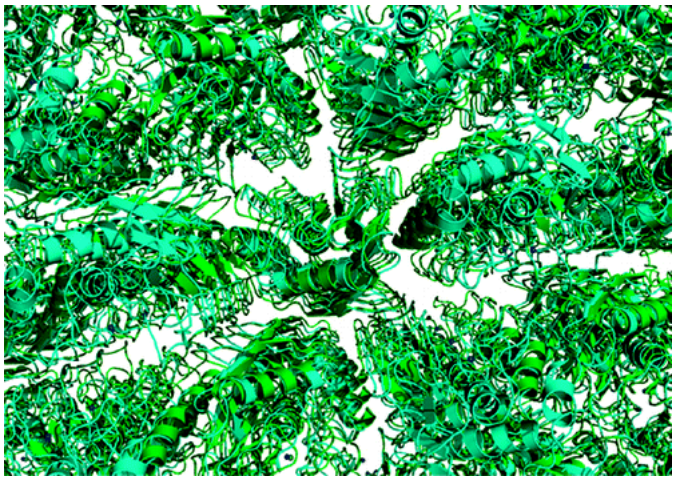

Pseudocontact shifts (PCSs) measured by solid-state NMR spectroscopy (SS-NMR) on microcrystalline powders of a paramagnetic metalloprotein permit NMR crystallography. Along with other restraints for SS-NMR experiments, the protein molecular structure as well as the correct crystal packing are obtained.

- Thermoresponsive silver/polymer nanohybrids with switchable metal enhanced fluorescence
  Liu, J.; Li, A.; Tang, J.; Wang, R.; Kong, N.; Davis, T. P. *Chem. Commun.* **2012**, *48*, 4680-4682.
  Abstract:

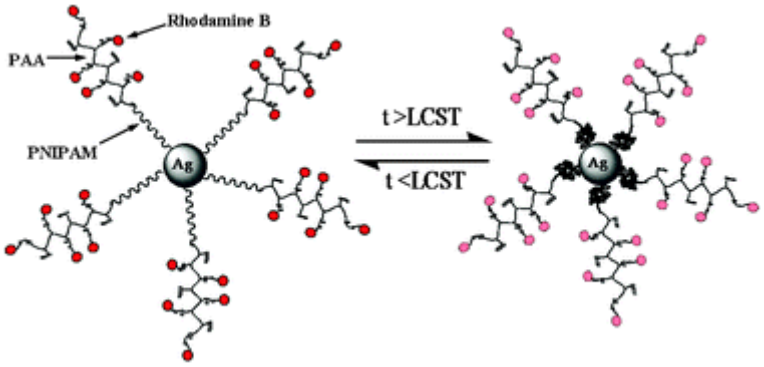

In this communication successful fabrication of fluorescent silver/polymer nanohybrids with thermo-switchable metal enhanced fluorescence (MEF) has been reported.

- Synthesis and characterization of ratiometric nanosensors for pH quantification: a mixed micelle approach
  Kumar, E. K. P.; Almdal, K.; Andresen, T. L. *Chem. Commun.* **2012**, *48*, 4776-4778.
  Abstract:

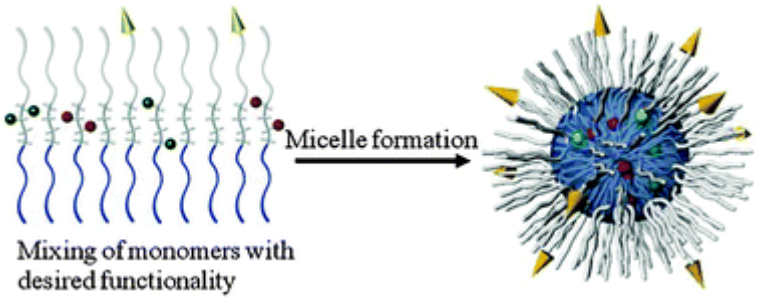

Nanosensor synthesis by self-assembly of functionalized triblock copolymers provides a nanometre sized micelle. This new method provides high flexibility in sensor design and in optimization of sensor properties.

- Synthesis and optoelectronic properties of 2,6-bis(2-anilinoethynyl)pyridine scaffolds
  Engle, J.; Carroll, M. C. N.; Johnson, D. W.; Haley, M. M. *Chem. Sci.* **2012**, *3*, 1105-1110.
  Abstract:

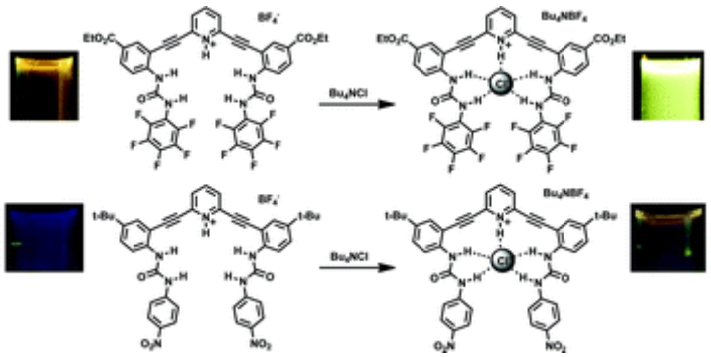

Synthesis and spectroscopic study of sixteen bisphenylureas demonstrate the fluorescence tunability inherent to these arylethynylpyridine-based anion sensors.

- How does a supramolecular polymeric nanowire form in solution?
  Lei, T.; Guo, Z. H.; Zheng, C.; Cao, Y.; Liang, D.; Pei, J.; *Chem. Sci.* **2012**, *3*, 1162-1168.
  Abstract:

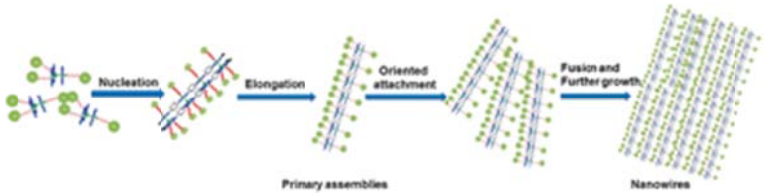

We demonstrate that after the supramolecular polymerization, the "oriented attachment" growth and fusion mechanism is another critical process for the formation of organic nanowires.

- Small-Molecule Photovoltaics Based on Functionalized Squaraine Donor Blends
  Xiao, X.; Wei, G.; Wang, S.; Zimmerman, J. D.; Renshaw, C. K.; Thompson, M. E.; Forrest, S. R. *Adv. Mater.* **2012**, *24*, 1956–1960.
  Abstract:

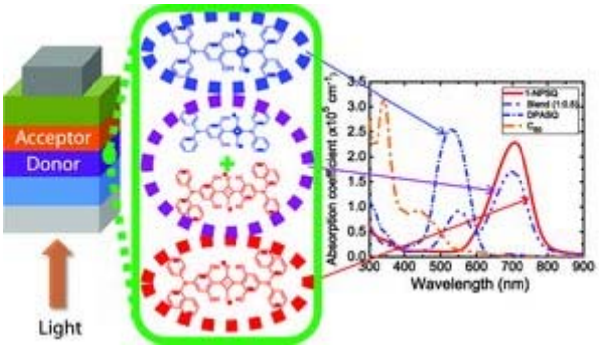

Two squaraine (SQ) donor molecules with different absorption bands are blended together for better coverage of the solar spectrum. The blend SQ device shows a significant improvement

compared with single SQ donor devices. By applying a solvent annealing process and a compound buffer layer, a power-conversion efficiency of 5.9 ± 0.3% is achieved under 1 sun illumination.

- Phosphorescent Organic Light-Emitting Diodes with Outstanding External Quantum Efficiency using Dinuclear Rhenium Complexes as Dopants
  Mauro, M.; Yang, C.-H.; Shin, C.-Y.; Panigati, M.; Chang, C.-H.; D'Alfonso, G.; De Cola, L. *Adv. Mater.* **2012**, *24*, 2054–2058.
  Abstract:

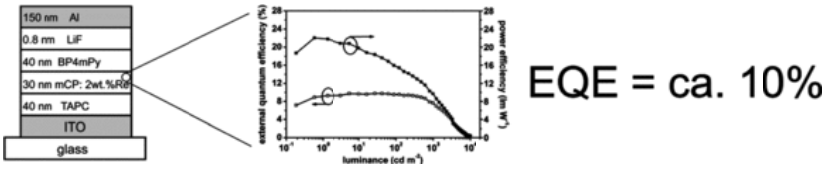

The photophysical and electroluminescence properties of two dinuclear rhenium(I) carbonyl complexes bearing 1,2-diazines are comprehensively investigated. The bromo-bridged complex is successfully used as triplet emitter for the preparation of vacuum-processed OLEDs with outstanding external quantum efficiencies, reaching a value of 10%.

- Intraribbon Heterojunction Formation in Ultranarrow Graphene Nanoribbons
  Blankenburg, S.; Cai, J.; Ruffieux, P.; Jaafar, R.; Passerone, D.; Feng, X.; Müllen, K.; Fasel, R.; Pignedoli, C. A. *ACS Nano* **2012,** *6*, 2020-2025.
  Abstract:

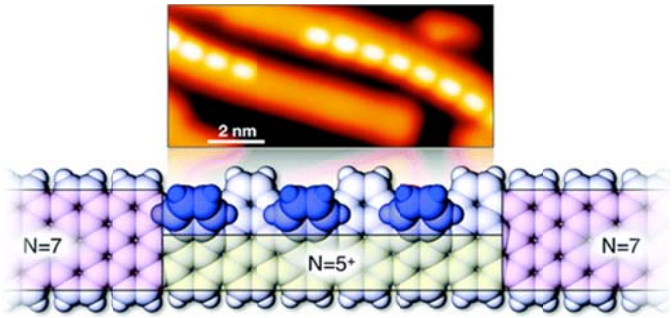

Graphene nanoribbons—semiconducting quasi-one-dimensional graphene structures—have great potential for the realization of novel electronic devices. Recently, graphene nanoribbon heterojunctions—interfaces between nanoribbons with unequal band gaps—have been realized with lithographic etching techniques and *via* chemical routes to exploit quantum transport phenomena. However, standard fabrication techniques are not suitable for ribbons narrower than 5 nm and do not allow to control the width and edge structure of a specific device with atomic precision. Here, we report the realization of graphene nanoribbon heterojunctions with lateral dimensions below 2 nm *via* controllable dehydrogenation of polyanthrylene oligomers self-assembled on a Au(111) surface from molecular precursors. Atomistic simulations reveal the microscopic mechanisms responsible for intraribbon heterojunction formation. We demonstrate the capability to selectively modify the heterojunctions by activating the dehydrogenation reaction on single units of the nanoribbons by electron injection from the tip of a scanning tunneling microscope.

- Surface-Engineered Gold Nanorods: Promising DNA Vaccine Adjuvant for HIV-1 Treatment
  Xu, L.; Liu, Y.; Chen, Z.; Li, W.; Liu, Y.; Wang, L.; Liu, Y.; Wu, X.; Ji, Y.; Zhao, Y.; Ma, L.; Shao, Y.; Chen, C. *Nano Letters* **2012**, *12*, 2003-2012.

Abstract:

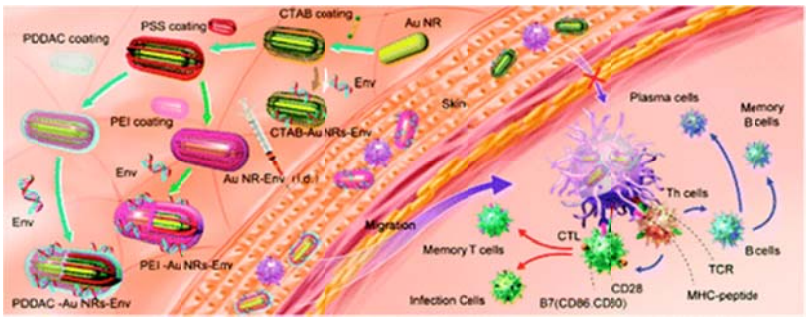

With the intense international response to the AIDS pandemic, HIV vaccines have been extensively investigated but have failed due to issues of safety or efficacy in humans. Adjuvants for HIV/AIDS vaccines are under intense research but a rational design approach is still lacking. Nanomaterials represent an obvious opportunity in this field due to their unique physicochemical properties. Gold nanostructures are being actively studied as a promising and versatile platform for biomedical application. Herein, we report novel surface-engineered gold nanorods (NRs) used as promising DNA vaccine adjuvant for HIV treatment. We have exploited the effects of surface chemistry on the adjuvant activity of the gold nanorod by placing three kinds of molecules, that is, cetyltrimethylammonium bromide (CTAB), poly(diallydimethylammonium chloride) (PDDAC), and polyethyleneimine (PEI) on the surface of the nanorod. These PDDAC- or PEI-modified Au NRs can significantly promote cellular and humoral immunity as well as T cell proliferation through activating antigen-presenting cells if compared to naked HIV-1 Env plasmid DNA treatment in vivo. These findings have shed light on the rational design of low-toxic nanomaterials as a versatile platform for vaccine nanoadjuvants/delivery systems.

- Light trapping structures in wing scales of butterfly *Trogonoptera brookiana*
  Han, Z.; Niu, S.; Shang, C.; Liu, Z.; Ren, L. *Nanoscale* **2012**, *4*, 2879-2883.
  Abstract:

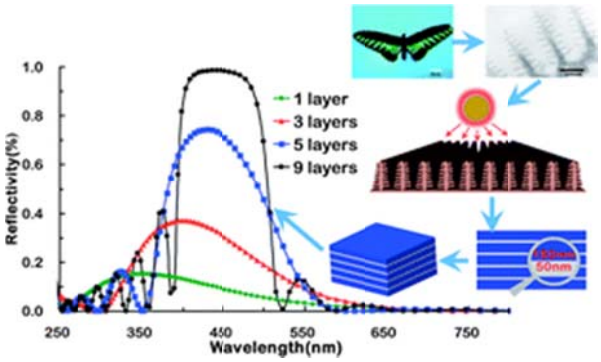

The fine optical structures in wing scales of *Trogonoptera brookiana*, a tropical butterfly exhibiting efficient light trapping effect, were carefully examined and the reflectivity was measured using reflectance spectrometry. The optimized 3D configuration of the coupling structure was determined using SEM and TEM data, and the light trapping mechanism of butterfly scales was studied. It is found that the front and back sides of butterfly wings possess different light trapping structures, but both can significantly increase the optical path and thus result in almost total absorption of all incident light. An optical model was created to check the properties of this light trapping structure. The simulated reflectance spectra are in concordance with the experimental ones. The results reliably confirm that these structures induce efficient light trapping effect. This functional "biomimetic structure" would have a potential value in wide engineering and optical applications.

- A Sensitive Zinc-Activated 129Xe MRI Probe
  Kotera, N.; Tassali, N.; Léonce, E.; Boutin, C.; Berthault, P.; Brotin, T.; Dutasta, J.-P.; Delacour, L.; Traoré, T.; Buisson, D.-A.; Taran, F.; Coudert, S.; Rousseau, B. *Angew. Chem. Int. Ed.* **2012**, *51*, 4100-4103.
  Abstract:

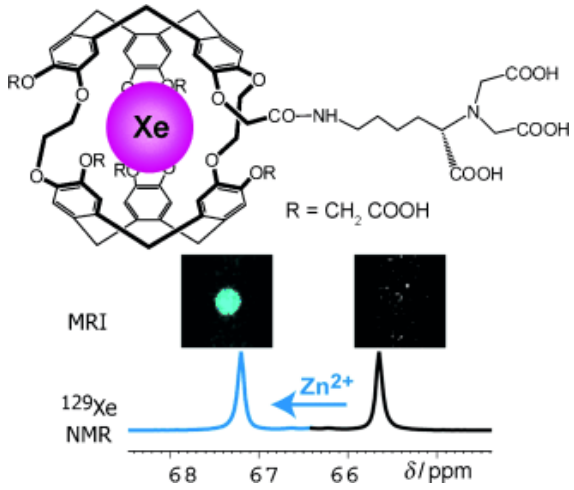

Xenon capsule: A smart ^{129}Xe NMR-based sensor of Zn^{2+} ions for magnetic resonance imaging (MRI) is proposed. The resonance frequency of xenon encapsulated in a cryptophane that bears a nitrilotriacetic ligand moiety varies when Zn^{2+} ions are present in solution (see picture). With hyper-polarized gas, such a construct enables detection of 100 nM zinc in one xenon batch, a threshold 300 times lower than achieved with gadolinium chelates.

- Sequential, Kinetically Controlled Synthesis of Multicomponent Stereoisomeric Assemblies
  Chepelin, O.; Ujma, J.; Barran, P. E.; Lusby, P. J. *Angew. Chem. Int. Ed.* **2012**, *51*, 4194-4197.
  Abstract:

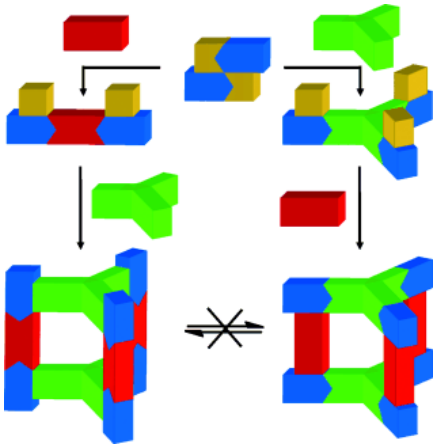

In control: Multicomponent stereoisomeric assemblies have been synthesized from asymmetric cyclometalated platinum corner units that have exchangeable *cis* coordination sites with different labilities. A template-free, kinetically controlled approach resulted in the selective formation of trigonal prismatic isomers by changing the sequence of addition of 4,4'-bipyridine (red) and tris(4-pyridyl)triazine (green) to [(**L**Pt)$_2$Cl$_2$] (blue and yellow; H**L** = 2-phenylpyridine).

- Naphthodithiophene-Based Donor–Acceptor Polymers: Versatile Semiconductors for OFETs and OPVs
  Osaka, I.; Abe, T.; Shimawaki, M.; Koganezawa, T.; Takimiya, K. *ACS Macro Lett.* **2012**, *1*, 437–440.
  Abstract:

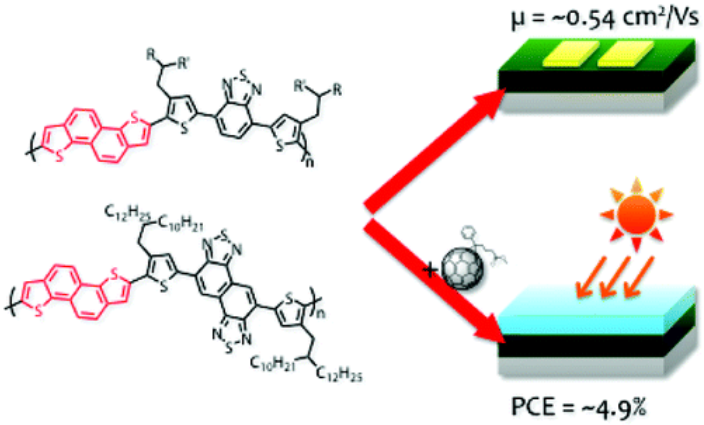

We report the synthesis, characterization, and OFET and OPV properties of a series of novel naphthodithiophene (NDT3)-based donor–acceptor semiconducting polymers. A striking feature of the present polymers is the very close π–π stacking of 3.5 Å, most likely as a result of the large π system and the D–A system in the polymer backbone. PNDT3NTz-DT, in particular, is found to be one of the few examples of versatile polymers that exhibit both the field-effect mobility of ~0.5 $cm^2/(V\ s)$ and the PCE of ~5%. These results indicate that NDT3 is a promising versatile core unit for semiconducting polymers and that the use of highly π-extended heteroarenes as both the donor and the acceptor unit is a promising design strategy to develop high performance polymers.

- Effect of *o*-Carborane on the Optoelectronic and Device-Level Properties of Poly(fluorene)s
  Davis, A. R.; Peterson, J. J.; Carter, K. R. *ACS Macro Lett.* **2012**, *1*, 469–472.
  Abstract:

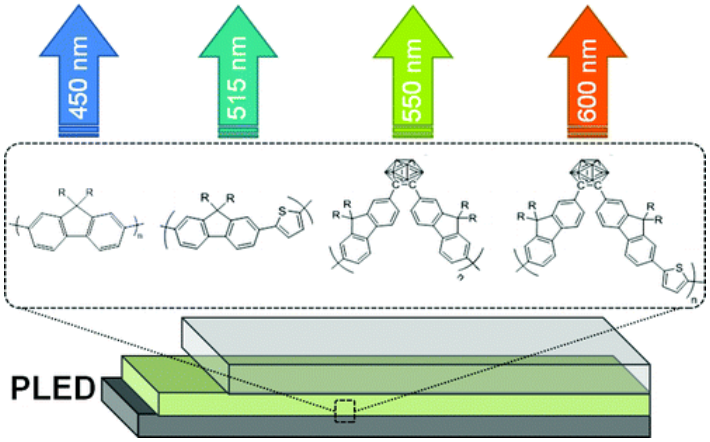

Carboranes have been previously noted to distinctively affect the luminescent properties of semiconducting polymers when incorporated into the conjugated backbone. In this report, we use carborane-based poly(fluorene) derivatives as active materials for polymer light-emitting diodes and transistors. Optoelectronic analysis unequivocally shows that carborane does not participate in the π-conjugated network, yet their presence causes major red-shifting in device electroluminescence as well as in thin film photoluminescence. In field effect transistors, they also improve charge carrier mobility by an order of magnitude despite disrupting π-conjugation. This use of carborane-containing

conjugated polymers in active devices holds promise as new responsive materials in electronic polymer applications.

- Nanochannels: Hosts for the Supramolecular Organization of Molecules and Complexes
  Calzaferri, G.*Langmuir* **2012**, *28*, 6216–6231.
  Abstract:

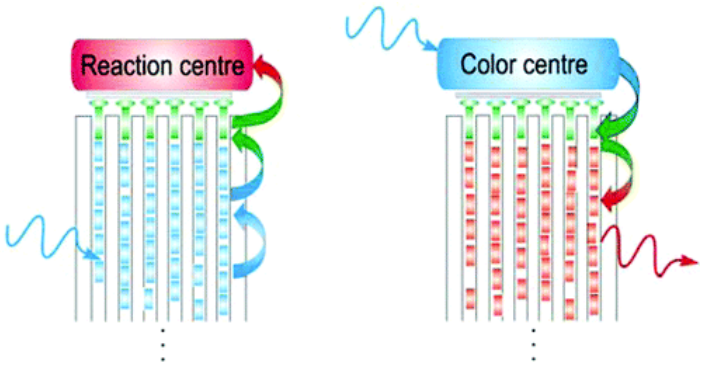

Nanochannels have been used as hosts for supramolecular organization for a large variety of guests. The possibilities for building complex structures based on 2D and especially 3D nanochannel hosts are larger than those based on 1D nanochannel hosts. The latter are, however, easier to understand and to control. They still give rise to a rich world of fascinating objects with very distinguished properties. Important changes are observed if the channel diameter becomes smaller than 10 nm. The most advanced guest–nanochannel composites have been synthesized with nanochannels bearing a diameter of about 1 nm. Impressive complexity has been achieved by interfacing these composites with other objects and by assembling them into specific structures. This is explained in detail. Guest–nanochannel composites that absorb all light in the right wavelength range and transfer the electronic excitation energy via FRET to well-positioned acceptors offer a unique potential for developing FRET-sensitized solar cells, luminescent solar concentrators, color-changing media, and devices for sensing in analytical chemistry, biology, and diagnostics. Successful 1D nanochannel hosts for synthesizing guest–host composites have been zeolite-based. Among them the largest variety of guest–zeolite composites with appealing photochemical, photophysical, and optical properties has been prepared by using zeolite L (ZL) as a host. The reasons are the various possibilities for fine tuning the size and morphology of the particles, for inserting neutral molecules and cations, and for preparing rare earth complexes inside by means of the ship-in-a-bottle procedure. An important fact is that the channel entrances of ZL-based composites can be functonalized and completely blocked, if desired, and furthermore that targeted functionalization of the coat is possible. Different degrees of organizational levels and prospects for applications are discussed, with special emphasis on solar energy conversion devices.

- Role of the Triiodide/Iodide Redox Couple in Dye Regeneration in p-Type Dye-Sensitized Solar Cells
  Gibson, E. A.; Le Pleux, L.; Fortage, J.; Pellegrin, Y.; Blart, E.; Odobel, F.; Hagfeldt, A.; Boschloo, G.*Langmuir* **2012**, *28*, 6485–6493.
  Abstract:

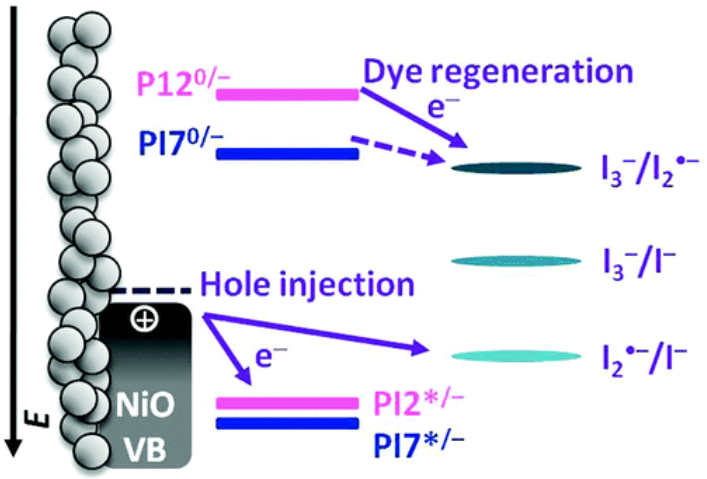

A series of perylene dyes with different optical and electronic properties have been used as photosensitizers in NiO-based p-type dye-sensitized solar cells. A key target is to develop dyes that absorb light in the red to near-infrared region of the solar spectrum in order to match photoanodes optically in tandem devices; however, the photocurrent produced was found to decrease dramatically as the absorption maxima of the dye used was varied from 517 to 565 nm and varied strongly with the electrolyte solvent (acetonitrile, propionitrile, or propylene carbonate). To determine the limitations of the energy properties of the dye molecules and to provide guidelines for future sensitizer design, we have determined the redox potentials of the diiodide radical intermediate involved in the charge-transfer reactions in different solvents using photomodulated voltammetry. $E°(I_3^-/I_2^{\bullet-})$ (V vs $Fe(Cp)_2^{+/0}$) = −0.64 for propylene carbonate, −0.82 for acetonitrile, and −0.87 for propionitrile. Inefficient regeneration of the sensitizer appears to be the efficiency-limiting step in the device, and the values presented here will be used to design more efficient dyes, with more cathodic reduction potentials, for photocathodes in tandem dye-sensitized solar cells.

- Self-Assembled Organic Nanotubes through Instant Gelation and Universal Capacity for Guest Molecule Encapsulation
  Cao, H.; Duan, P.; Zhu, X.; Jiang, J.; Liu, M. *Chem. Eur. J.* **2012**, *18*, 5546 – 5550.
  Abstract:

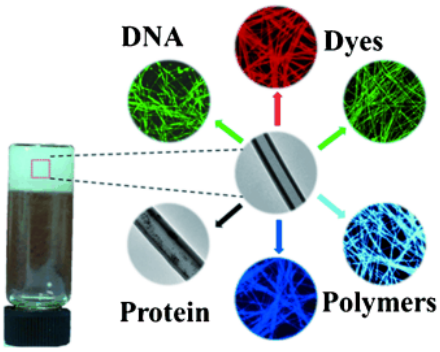

A C_3 symmetrical L-glutamic acid based gelator was found to instantly form hexagonal nanotubes through anti-solvent gelation in a wide range of mixed solvents at room temperature. Guest molecules, including simple dyes and biological macromolecules, could be entrapped in the nanotubes (see figure). This method provides a general and efficient way for the encapsulation of guest compounds in organic nanotubes.

- Accelerating the Multifunctionalization of Therapeutic Nanoparticles by Using a

Multicomponent Reaction

Zhou, H.; Su, G.; Jiao, P.; Yan, B. *Chem. Eur. J.* **2012**, *18*, 5501 – 5505.

Abstract:

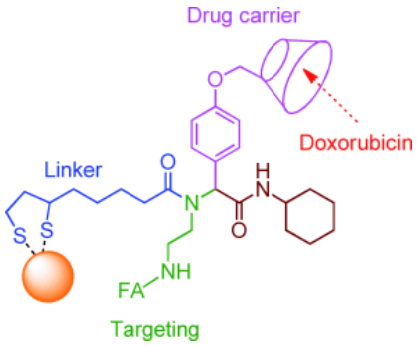

Multifunctionalized nanoparticles are crucial for nanobiomedical applications, but their syntheses are tedious and time-consuming. A multicomponent reaction on nanostructures is an excellent way to prepare such nanomaterials. The gold nanosystem illustrated in the scheme was built and shown to enhance cancer cell targeting and killing by combining the effects of a therapeutic drug with X-ray radiation.

- Enantioselective C-H Crotylation of Primary Alcohols via Hydrohydroxyalkylation of Butadiene

  Zbieg, J. R.; Yamaguchi, E.; McInturff, E. L.; Krische, M. J. *Science* **2012**, *336*, 324-327.

  Abstract:

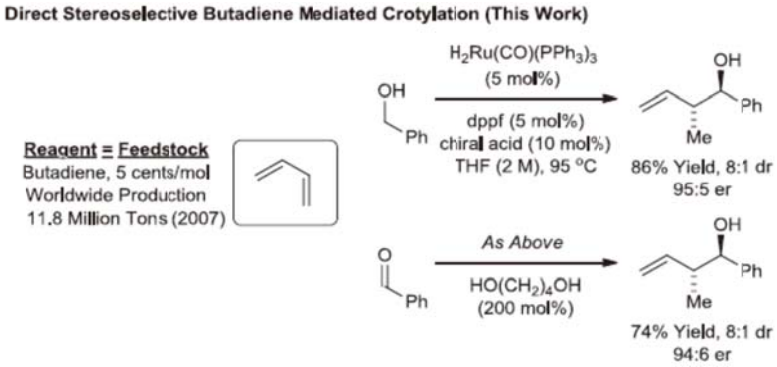

The direct, by-product-free conversion of basic feedstocks to products of medicinal and agricultural relevance is a broad goal of chemical research. Butadiene is a product of petroleum cracking and is produced on an enormous scale (about 12 × 106 metric tons annually). Here, with the use of a ruthenium catalyst modified by a chiral phosphate counterion, we report the direct redox-triggered carbon-carbon coupling of alcohols and butadiene to form products of carbonyl crotylation with high levels of anti-diastereoselectivity and enantioselectivity in the absence of stoichiometric by-products.

- Biosynthetic pathway toward carbohydrate-like moieties of alnumycins contains unusual steps for C-C bond formation and cleavage.

  Ojaa, T.; Klikab, K. D.; Appassamya, L.; Sinkkonenb, J.; Mäntsälää, P.; Niemia, J.; Metsä-Keteläa, M. *Proc. Nat. Acad. Sci. USA* **2012**, *109*, 6024-6029.

  Abstract:

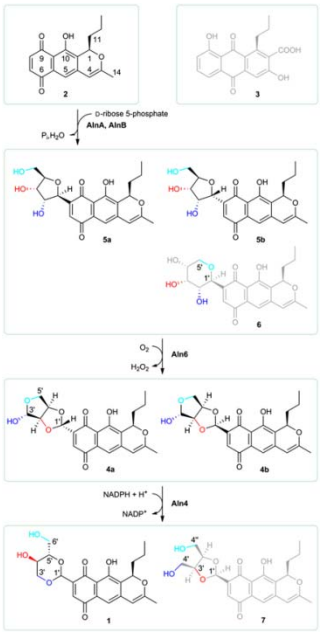

Carbohydrate moieties are important components of natural products, which are often imperative for the solubility and biological activity of the compounds. The aromatic polyketide alnumycin A contains an extraordinary sugar-like 4′-hydroxy-5′-hydroxymethyl-2′,7′-dioxane moiety attached via a carbon-carbon bond to the aglycone. Here we have extensively investigated the biosynthesis of the dioxane unit through ^{13}C labeling studies, gene inactivation experiments and enzymatic synthesis. We show that AlnA and AlnB, members of the pseudouridine glycosidase and haloacid dehalogenase enzyme families, respectively, catalyze C-ribosylation conceivably through Michael-type addition of D-ribose-5-phosphate and dephosphorylation. The ribose moiety may be attached both in furanose (alnumycin C) and pyranose (alnumycin D) forms. The $C_{1'}$-$C_{2'}$ bond of alnumycin C is subsequently cleaved and the ribose unit is rearranged into an unprecedented dioxolane (cisbicyclo[3.3.0]-2′,4′,6′-trioxaoctan-3′β-ol) structure present in alnumycin B. The reaction is catalyzed by Aln6, which belongs to a previously uncharacterized enzyme family. The conversion was accompanied with consumption of O_2 and formation of H_2O_2, which allowed us to propose that the reaction may proceed via hydroxylation of C1′ followed by retro-aldol cleavage and acetal formation. Interestingly, no cofactors could be detected and the reaction was also conducted in the presence of metal chelating agents. The last step is the conversion of alnumycin B into the final end-product alnumycin A catalyzed by Aln4, an NADPH-dependent aldo-keto reductase. This characterization of the dioxane biosynthetic pathway sets the basis for the utilization of C-C bound ribose, dioxolane and dioxane moieties in the generation of improved biologically active compounds.

- The 2.8 Å crystal structure of the dynein motor domain
  Kon, T.; Oyama, T.; Shimo-Kon, R.; Imamula, K.; Shima, T.; Sutoh, K.; Kurisu, G. *Nature* **2012**, *484*, 345-350.
  Abstract:

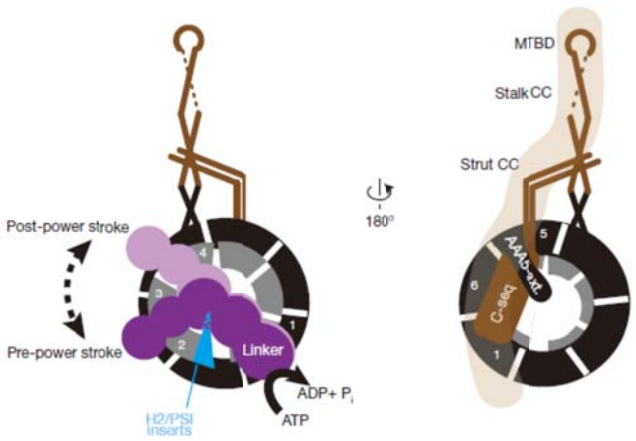

Dyneins are microtubule-based AAA$^+$ motor complexes that power ciliary beating, cell division, cell migration and intracellular transport. Here we report the most complete structure obtained so far, to our knowledge, of the 380-kDa motor domain of Dictyostelium discoideum cytoplasmic dynein at 2.8 Å resolution; the data are reliable enough to discuss the structure and mechanism at the level of individual amino acid residues. Features that can be clearly visualized at this resolution include the coordination of ADP in each of four distinct nucleotide-binding sites in the ring-shaped AAA$^+$ ATPase unit, a newly identified interaction interface between the ring and mechanical linker, and junctional structures between the ring and microtubule-binding stalk, all ofwhich should be critical for the mechanism of dynein motility. We also identify a long-range allosteric communication pathway between the primary ATPase and the microtubule-binding sites. Our work provides a framework for understanding the mechanism of dynein-based motility.

- Integrated 3D-printed reactionware for chemical synthesis and analysis
  Symes, M. D.; Kitson, P. J.; Yan, J.; Richmond, C. J.; Cooper, G. J. T.; Bowman, R.; Vilbrandt, T.; Cronin, L. *Nature Chemistry* **2012**, *4*, 349–354.
  Abstract:

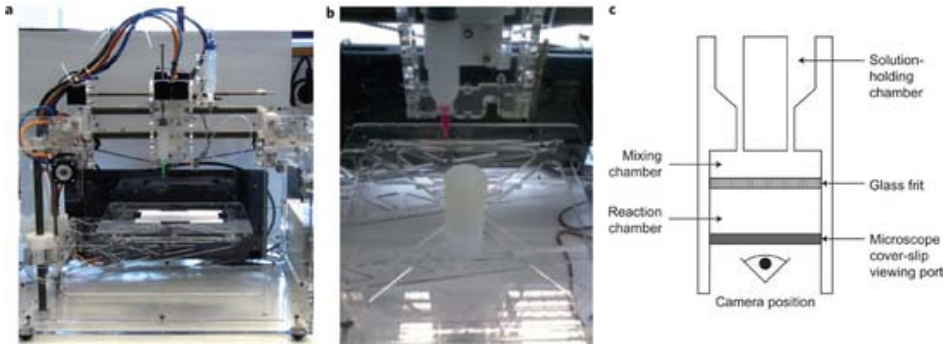

Three-dimensional (3D) printing has the potential to transform science and technology by creating bespoke, low-cost appliances that previously required dedicated facilities to make. An attractive, but unexplored, application is to use a 3D printer to initiate chemical reactions by printing the reagents directly into a 3D reactionware matrix, and so put reactionware design, construction and operation under digital control. Here, using a low-cost 3D printer and open-source design software we produced reactionware for organic and inorganic synthesis, which included printed-in catalysts and other architectures with printed-in components for electrochemical and spectroscopic analysis. This enabled reactions to be monitored in situ so that different reactionware architectures could be screened for their efficacy for a given process, with a digital feedback mechanism for device optimization. Furthermore, solely by modifying reactionware architecture, reaction outcomes can be

altered. Taken together, this approach constitutes a relatively cheap, automated and reconfigurable chemical discovery platform that makes techniques from chemical engineering accessible to typical synthetic laboratories.

- Ultrathin and lightweight organic solar cells with high flexibility
  Kaltenbrunner, M.; White, M. S.; Głowacki, E. D.; Sekitani, T.; Someya, T.; Sariciftci, N. S.; Bauer, S. *Nature Communications* **2012***, 3*, 770.
  Abstract:

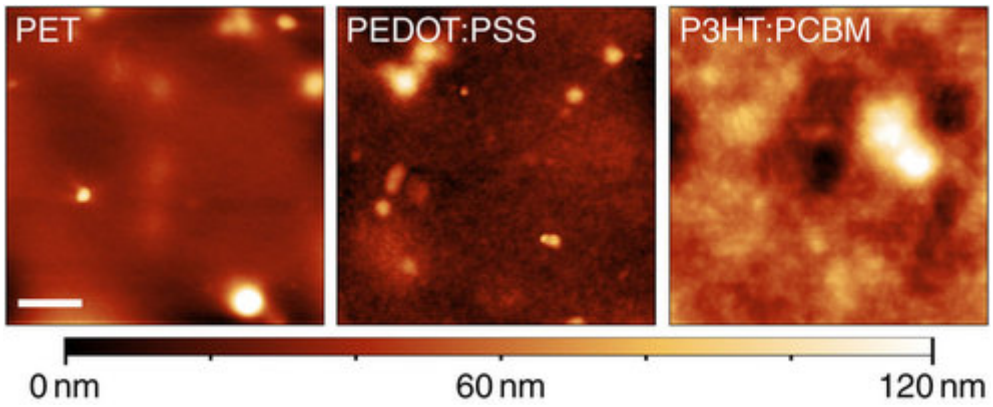

Application-specific requirements for future lighting, displays and photovoltaics will include large-area, low-weight and mechanical resilience for dual-purpose uses such as electronic skin, textiles and surface conforming foils. Here we demonstrate polymer-based photovoltaic devices on plastic foil substrates less than 2 µm thick, with equal power conversion efficiency to their glass-based counterparts. They can reversibly withstand extreme mechanical deformation and have unprecedented solar cell-specific weight. Instead of a single bend, we form a random network of folds within the device area. The processing methods are standard, so the same weight and flexibility should be achievable in light emitting diodes, capacitors and transistors to fully realize ultrathin organic electronics. These ultrathin organic solar cells are over ten times thinner, lighter and more flexible than any other solar cell of any technology to date.

- Organic Conducting Polymer–Protein Interactions
  Higgins, M. J.; Molino, P. J.; Yue, Z.; Wallace, G. G. *Chem. Mater.* **2012**, *24*, 828–839.
  Abstract:

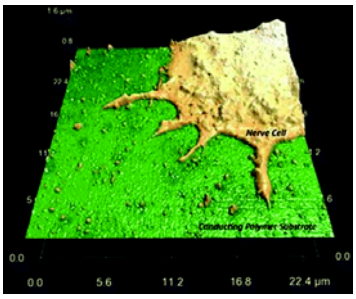

In this review, we provide insight into protein interactions with organic conducting polymers, a class of “intelligent” and dynamic materials that offer unique strategies for controlling protein interactions as a prelude to developing a wide range of bioapplications. Following a general introduction on the importance of protein interactions, this review initially focuses on the areas of bioseparation and biosensor applications. These applications amount to an extensive body of work; however, we provide only a brief overview for the purpose of introducing palpable examples of translating the

ability to control organic conducting polymer–protein interactions into practical and useful applications. Because organic conducting polymers are breaking new ground for implantable electrodes and tissue regeneration/engineering, we duly turn to the importance of protein interactions and role organic conducting polymers can play in advancing these applications. Lastly, for those not familiar with organic conducting polymers, we take a step back and examine the unique properties underlying their innate ability to control protein interactions, particularly the use of external electrical control to reversibly switch the physical surface properties. Several characterization techniques identified as being critical to our understanding at the macroscopic down to the single molecule level are also highlighted.

- Naphthalene Diimide-Based Polymer Semiconductors: Synthesis, Structure–Property Correlations, and n-Channel and Ambipolar Field-Effect Transistors
  Guo, X.; Kim, F. S.; Seger, M. J.; Jenekhe, S. A.; Watson, M. D. *Chem. Mater.* **2012**, *24*, 1434–1442.
  Abstract:

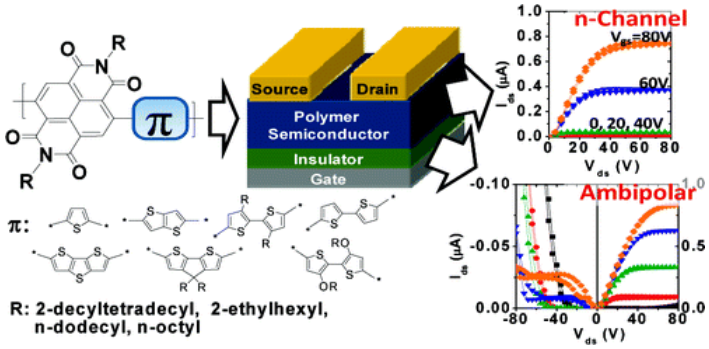

A series of nine alternating donor–acceptor copolymer semiconductors based on naphthalene diimide (NDI) acceptor and seven different thiophene moieties with varied electron-donating strength and conformations has been synthesized, characterized, and used in n-channel and ambipolar organic field-effect transistors (OFETs). The NDI copolymers had moderate to high molecular weights, and most of them exhibited moderate crystallinity in thin films and fibers. The LUMO energy levels of the NDI copolymers, at −3.9 to −3.8 eV, were constant as the donor moiety was varied. However, the HOMO energy levels could be tuned over a wide range from −5.3 eV in **P8** to −5.9 eV in **P1** and **P3**. As semiconductors in n-channel OFETs with gold source/drain electrodes, the NDI copolymers exhibited good electron transport with maximum electron mobility of 0.07 $cm^2/(V\ s)$ in **P5**. Although head-to-head (HH) linkage induced backbone torsion, polymer **P4** showed substantial electron mobility of 0.012 $cm^2/(V\ s)$ in bottom-gate/top-contact device geometry. Some of the copolymers with high-lying HOMO levels (**P7** and **P8**) exhibited ambipolar charge transport in OFETs with high electron mobilities (0.006–0.02 $cm^2/(V\ s)$) and significant hole mobilities ($>10^{-3}$ $cm^2/(V\ s)$). Varying the device geometry from top-contact to bottom-contact leads to the appearance or enhancement of hole transport in **P4**, **P6**, **P7**, and **P8**. Copolymers with smaller alkyl side chains on the imide group of NDI have enhanced carrier mobilities than those with bulkier alkyl side chains. These results show underlying structure–property relationships in NDI-based copolymer semiconductors while demonstrating their promise in n-channel and ambipolar transistors.